Applied Physics B (2019) 125:131
https://doi.org/10.1007/s00340-019-7246-4

Applied Physics B
Lasers and Optics

Passively Q-switched laser action of Yb:LaCa$_4$O(BO$_3$)$_3$ crystal at 1.07–1.08 μm induced by 2D Bi$_2$Te$_3$ topological insulator

Yuhang Li[1] · Meijie Liu[1] · Junxian Chen[1] · Liang Dong[1] · Jingnan Yang[1] · Junhai Liu[1]

Received: 1 May 2019 / Accepted: 19 June 2019 / Published online: 24 June 2019

Abstract

Efficient passively Q-switched laser operation of Yb:LaCa$_4$O(BO$_3$)$_3$ crystal was realized at the long-wavelength region of 1071–1080 nm, with 2D Bi$_2$Te$_3$ topological insulator acting as saturable absorber. With an incident pump power of 6.89 W, 1.76 W of pulsed output power was generated at 140 kHz with a slope efficiency of 38%; the corresponding pulse energy, duration, and peak power were, respectively, 12.6 μJ, 288 ns, and 43.8 W.

1 Introduction

Most Yb-ion lasers, without wavelength selecting, operate in the 1.02–1.07 μm spectral region, with long-wavelength oscillation beyond 1.07 μm being relatively rare. This is particularly the case for Q-switched Yb-ion lasers, where large output couplings are usually employed, forcing laser oscillation to shift toward short-wavelength side. For instance, despite the fact that both the Yb:YCa$_4$O(BO$_3$)$_3$ (Yb:YCOB) and the Yb:GdCa$_4$O(BO$_3$)$_3$ (Yb:GdCOB) crystal lasers are capable of emitting at wavelengths longer than 1.08 μm in free-running mode [1–3], their Q-switched operations, either actively with acousto-optic modulator [4, 5], or passively with Cr^{4+}:YAG [6, 7], with GaAs [8–10], with two-dimensional (2D) transition metal dichalcogenides [11, 12], or with 2D topological insulators [13, 14], were all demonstrated in a short-wavelength range of 1020–1045 nm. Only in a very special case of an Yb:YCOB laser passively Q-switched with InGaAs quantum wells, where the reflectivity of the output coupler used was as high as 97.5% (output coupling of 2.5%), could pulsed laser radiation be produced at long wavelengths around 1086 nm [15].

Laser radiation near 1.08 μm has been known to have some special practical applications in earth detection and in medical treatment. In addition, visible laser sources operating at about 540 nm can also be made by the use of the second-harmonic generation technique, which are of particular importance in cosmetology and in blood examination [16].

Among the Yb-ion laser crystals developed thus far, the monoclinic rare-earth calcium oxyborates, represented by Yb:YCOB and Yb:GdCOB, turn out to be quite unique for their large Stark splitting of the $^2F_{7/2}$ ground state (> 1000 cm^{-1} [17, 18]), which enables long-wavelength laser operation. Besides Yb:YCOB and Yb:GdCOB, which were intensively investigated, there exists a third member in this class of oxyborates, Yb:LaCa$_4$O(BO$_3$)$_3$ (Yb:LaCOB), of which the studies remained very limited in the past long period after its first appearance [17]. In fact, even the continuous-wave output power produced with Yb:LaCOB crystal is still limited to 2–3 W level [19, 20].

Very recently, we demonstrated a passively Q-switched Yb:LaCOB laser operating at wavelengths of 1031–1039 nm, with 2D MoTe$_2$ acting as saturable absorber [21]. Similar to the case of Yb:YCOB or Yb:GdCOB, the emission spectrum of Yb:LaCOB also consists of, apart from a main emission band around 1029 nm, a long-wavelength sideband having its peak at 1077 nm [22], it is, therefore, feasible to realize laser operation in this long-wavelength region.

In this paper, we report on passively Q-switched laser operation of Yb:LaCOB crystal at 1071–1080 nm. With a specially designed reflector mirror utilized in the laser resonator, the high-gain short-wavelength oscillation in the main emission band was successfully suppressed. The passive Q-switching action was induced by incorporating a 2D Bi$_2$Te$_3$ topological insulator into the laser resonator to act as a saturable absorber. To our knowledge, this was the first time an Yb-ion laser passively Q-switched with 2D saturable

✉ Junhai Liu
junhai_liu@hotmail.com

[1] College of Physics, Qingdao University, Ning-Xia Road 308, Qingdao 266071, China

absorber was demonstrated in the long-wavelength region beyond 1.07 µm.

2 Description of experiment

The Yb:LaCOB crystal sample used in the experiment was cut along the X principal optic axis, it was 6.0 mm long, with a square aperture of 3.0 mm × 3.0 mm, the Yb-ion concentration of the crystal was 22.5 at.%. The 2D Bi_2Te_3 sample was prepared on a 0.35 mm-thick sapphire substrate by chemical vapor deposition (CVD) technique. The absorption saturation properties of this 2D Bi_2Te_3 sample were measured in our previous work, giving I_{sat} (saturation intensity) = 2.12 MW/cm^2, ΔT (modulation depth) = 1.3%, and A_{ns} (non-saturable loss) = 53.9% [14]. In our experiment, a compact plane-parallel resonator was employed to build the passively Q-switched Yb:LaCOB/Bi_2Te_3 laser. To suppress the main emission band oscillation, the plane reflector mirror was coated for high transmittance at 950–1055 nm ($T > 90\%$) and for high reflectance at 1070–1150 nm ($R > 99.5\%$). For output coupler, a group of plane mirrors with transmittance (output coupling) ranging from $T = 10$ to 60% were utilized. Inside the resonator, the Yb:LaCOB crystal sample was placed close to the plane reflector, while the 2D Bi_2Te_3 sample was positioned between the laser crystal and the plane output coupler, leaving a total cavity length (physical) of 8.0 mm. As pump source, a fiber-coupled diode laser, with fiber core diameter of 105 µm and NA of 0.22, was utilized. It was capable of producing a maximum output power of 25 W at 975 nm with a bandwidth of less than 0.5 nm. The pump radiation was focused first and then delivered onto the Yb:LaCOB crystal, with a pump spot radius of approximately 70 µm.

3 Results and discussion

With the compact plane-parallel resonator that was formed using the specific reflector mirror, oscillation in the main emission band of Yb:LaCOB could be completely suppressed, and stable passively Q-switched laser action was realized at the long-wavelength region of 1071–1080 nm, for output couplings in the range of $T = 30$–50%. Under conditions of lower output coupling, $T \leq 20\%$, the pulsed output power generated in stable Q-switched operation was limited to less than 0.5 W, while higher output couplings of $T \geq 60\%$ also proved to be unsuitable owing to the too high lasing threshold.

Figure 1 shows the pulsed output power versus incident pump power (P_{in}) for three output couplings of $T = 30\%$, 40%, and 50%. The laser radiation was linearly polarized with **E**//Z, independent of the output coupling as well as

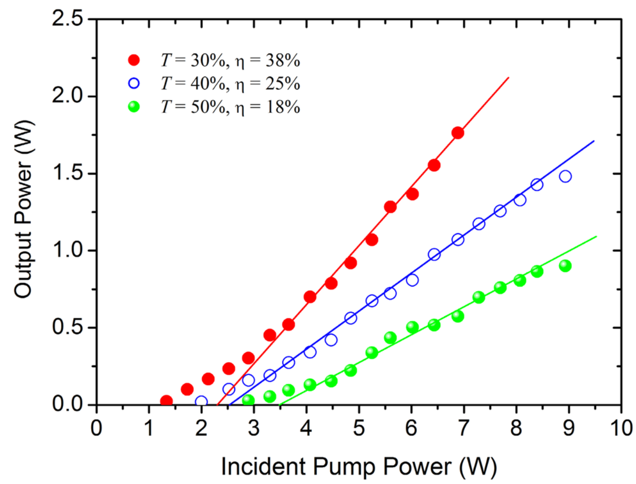

Fig. 1 Pulsed output power versus incident pump power for different output couplings of $T = 30$, 40, and 50%

the pumping level. The fraction of incident pump power absorbed by the 6 mm long X-cut Yb:LaCOB crystal sample was measured under non-lasing conditions to be $\eta_a = 0.95$ (small-signal or unsaturated value). In the case of $T = 30\%$, the Q-switched lasing threshold was reached at $P_{in} = 1.20$ W. Above the threshold, the pulsed output power increased with pump power, reaching 1.76 W at $P_{in} = 6.89$ W, and the optical-to-optical efficiency was 25.5%. The slope efficiency, determined over the high pump power region of $P_{in} > 3.5$ W, amounted to 38%. With the pump power raised in excess of $P_{in} = 6.89$ W, the Q-switched laser operation would deteriorate, arising from the increasingly strengthened thermal effects in the 2D Bi_2Te_3 sample. As the output coupling of the laser resonator was increased to $T = 40\%$, the lasing threshold also became increased, it was measured as $P_{in} = 1.95$ W. Besides the threshold rising, the pulsed laser action proved to be less efficient in this case, with the slope efficiency determined to be 25%, considerably lower than for $T = 30\%$. On the other hand, however, the pump range, over which stable pulsed laser operation could be achieved, turned out to be significantly wider than in the case of $T = 30\%$; the applicable pump power could be extended to $P_{in} = 8.93$ W, at which the pulsed output power generated was 1.48 W. The wider operational region attainable in the case of higher output coupling, might be attributed to the lower intracavity circulating laser power, which could mitigate the Q-switching instability resulting from the thermal effects in the 2D Bi_2Te_3 absorber. With the output coupling further raised to $T = 50\%$, the pump power required for arriving at laser threshold increased to $P_{in} = 2.81$ W, and the Q-switched laser operation was found to be much less efficient, with the slope efficiency amounted only to 18%. Nonetheless, a maximum pulsed output power of 0.90 W could be produced prior to the onset of unstable Q-switching.

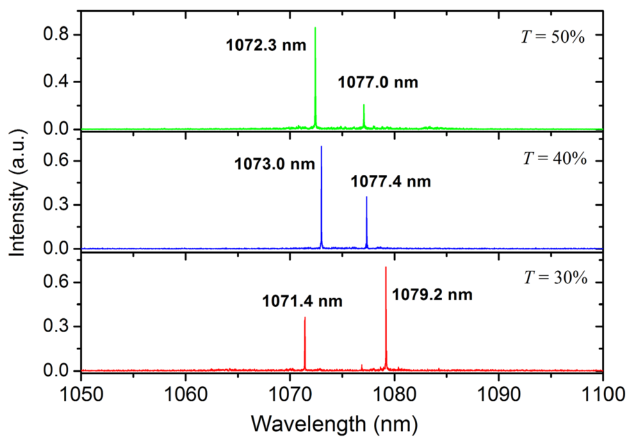

Fig. 2 Lasing spectrum measured at an incident pump power of 6.43 W for $T = 30$, 40, and 50%

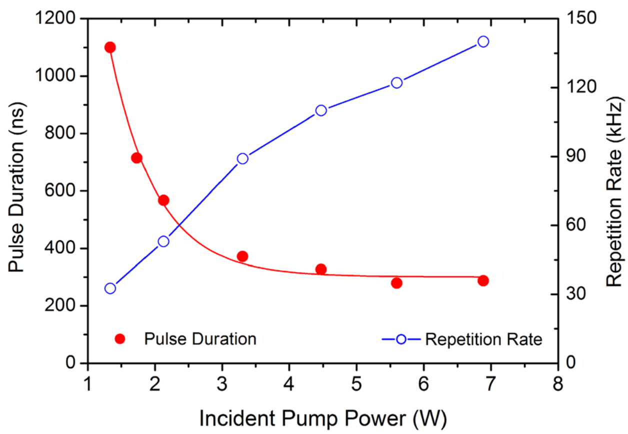

Fig. 3 Variation of pulse duration and repetition rate with incident pump power, measured for the case of $T = 30\%$

Figure 2 shows the laser emission spectra for $T = 30\%$, 40%, and 50%, which were measured at $P_{in} = 6.43$ W. It was found experimentally that the lasing spectrum of the Yb:LaCOB/Bi_2Te_3 laser, which was forced operating in the long-wavelength emission sideband, varied only slightly with the output coupling or with the pump power. One sees that the lasing wavelengths fell into the spectral region of 1071–1080 nm. One may also note a trend exhibited by the lasing spectrum, it would become wider with the output coupling decreased from $T = 50$ to 30%. The reason for this behavior is clear; as the overall resonator losses were lowered, the gain required for lasing would become less, making it possible for longitudinal modes in a wider emission band to oscillate.

Figure 3 depicts the pump power dependence of the pulse duration as well as the pulse repetition rate, measured for the case of $T = 30\%$. One notes that the pulse duration drops rapidly at the initial stage just above the Q-switching threshold; it then becomes shortened progressively with the increase of pump power, and eventually reaches a certain amount that will remain nearly unchanged. Such a varying behavior turns out to be typical of passive Q-switching induced by 2D Bi_2Te_3 and other 2D saturable absorbers [11–14, 21, 23]. Due to the high saturation intensity of the 2D Bi_2Te_3 sample, the part of the absorber that could be saturated just above threshold would be very limited, leading to a fairly wide pulse duration (longer than 1 μs); as the internal laser intensity increased with the rise of pump power, the saturation degree of the absorber would be enhanced increasingly, making the produced laser pulse shortened rapidly; then eventually, after the 2D Bi_2Te_3 sample could be saturated completely with the pump power increased to a sufficiently high level, the pulse duration would remain nearly unchanged, just as exhibited in an ordinary passive Q-switching induced by a traditional saturable absorber such as Cr^{4+}:YAG. The pulse duration measured at $P_{in} = 6.89$ W, where the highest output power was produced, was 288 ns, whereas the minimum duration, 279 ns, was achieved at $P_{in} = 5.60$ W. Similar variation behavior of pulse duration was also observed in the case of $T = 40\%$ or $T = 50\%$, and the shortest pulse duration obtained was 261 ns for $T = 40\%$ and 341 ns for $T = 50\%$.

As illustrated in Fig. 3, the pulse repetition rate reached just above the lasing threshold was fairly low, and it was measured to be 32.6 kHz at $P_{in} = 1.34$ W. With the pump power being raised, the repetition rate increased, reaching 140.0 kHz at the highest pump power ($P_{in} = 6.89$ W). The continuously increasing of the pulse repetition rate was simply because of the fact that as the pump power was raised, the time taken for the accumulation of population inversion that was required for compensating the overall resonator losses, would become shorter. For the case of $T = 40\%$

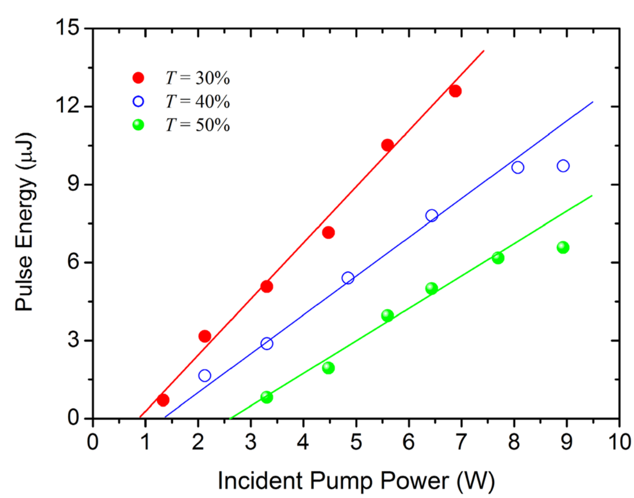

Fig. 4 Pulse energy versus incident pump power for $T = 30$, 40, and 50%

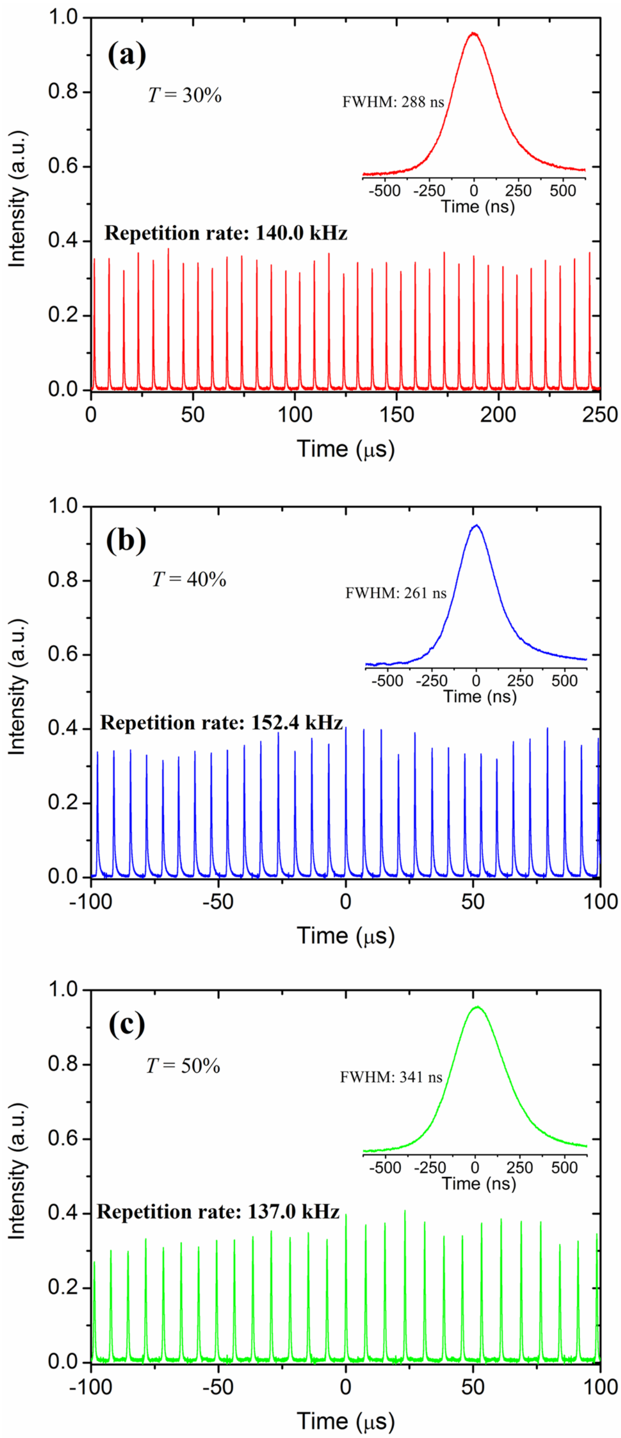

Fig. 5 Laser pulse train measured at $P_{in}=6.89$ W in the case of $T=30\%$ (**a**), at $P_{in}=8.90$ W in the case of $T=40\%$ (**b**), and at $P_{in}=8.90$ W in the case of $T=50\%$ (**c**). The temporal profile of an individual pulse is presented for each case as the inset

($T=50\%$), the repetition rate increased with pump power in a similar fashion, covering a range of 33.3–152.4 kHz (65.0–137.0 kHz).

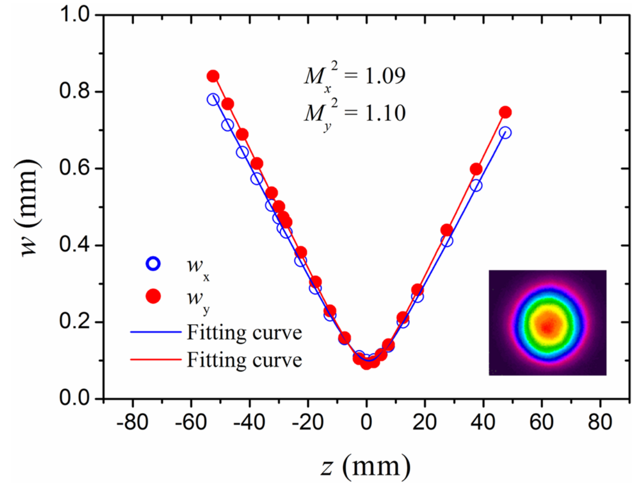

Fig. 6 Beam spot radius (w) versus propagation distance (z) measured for the horizontal (x) and vertical (y) directions. The inset shows a beam pattern

The pulse energy can be determined from the measured repetition rate and the corresponding pulsed output power. Figure 4 shows the pulse energy versus the incident pump power for $T=30\%$, 40%, and 50%. In the case of $T=30\%$, the pulse energy increased roughly linearly with pump power, reaching a maximum of 12.6 μJ at the highest pumping level. Given the pulse duration of 288 ns, the peak power reached was calculated to be 43.8 W. The largest pulse energies that were produced in the cases of $T=40\%$ and $T=50\%$ were, respectively, 9.7 and 6.6 μJ.

Figure 5a presents a pulse train measured at $P_{in}=6.89$ W in the case of $T=30\%$, showing a repetition rate of 140.0 kHz. The pulse amplitude fluctuations were determined as 2.2% (rms), while the timing jitters were 14.9% (rms). The temporal profile of an individual laser pulse is shown as the inset. Pulse trains generated in the cases of $T=40\%$ and $T=50\%$ were also measured at the highest pump power of $P_{in}=8.90$ W, which are shown in Fig. 5b ($T=40\%$) and Fig. 5c ($T=50\%$), the insets representing the individual pulse profiles.

The output beam quality of the Yb:LaCOB/Bi_2Te_3 laser was also examined. Figure 6 depicts the measured beam spot radius (w) as a function of the propagation distance (z) for the horizontal (x) and vertical (y) directions. The measurement was made at an output power of 1.5 W. Fitting the measured data in accordance with the Gaussian beam propagation law yields the beam quality factors: $M_x^2=1.09$, $M_y^2=1.10$. The inset presents a beam pattern.

Table 1 lists the principal parameters characterizing the passively Q-switched Yb:LaCOB/Bi_2Te_3 laser operating under the optimum output coupling of $T=30\%$. These parameters include: P_{max}, maximum pulsed output power; PRR, pulse repetition rate; E_p, pulse energy; t_p, pulse duration; P_p,

Table 1 Comparison of passive Q-switching performance induced by 2D Bi_2Te_3 in the Yb:LaCOB, Yb:YCOB, and Yb:GdCOB lasers

Laser	P_{max} (W)	E_p (µJ)	t_p (ns)	P_p (W)	η_s (%)	PRR range (kHz)	λ_l (nm)
Yb:LaCOB	1.76	12.6	288	43.8	38	32.6–140.0	1071–1080
Yb:YCOB[a]	3.85	9.63	96	100.3	28	110–400	1028–1037
Yb:GdCOB[b]	2.38	7.32	104	70.4	36	160–325	1031–1035

[a]From Ref. [13], for $T = 70\%$

[b]From Ref. [14], for $T = 50\%$

peak power; η_s, slope efficiency; and λ_l, lasing wavelength. For comparison, the results for the recently reported Yb:YCOB and Yb:GdCOB lasers, which were also passively Q-switched with 2D Bi_2Te_3-saturable absorber, but operated in the short-wavelength main emission band [13, 14], are also presented. One notices that the repetition rate, either the initial (lowest) or the final (highest), reached in the current Yb:LaCOB laser was much lower than for Yb:YCOB or Yb:GdCOB laser because of the much smaller emission cross section in the long-wavelength sideband ($<0.1\times10^{-20}$ cm^2 at 1077 nm, where the peak is located [22]). In addition, accordingly, higher pulse energy was obtained. In fact, the maximum attainable pulse energy, 12.6 µJ, produced by the Yb:LaCOB/Bi_2Te_3 laser, also proves to be the highest achieved so far with Yb- or Nd-ion lasers passively Q-switched by 2D Bi_2Te_3 or Bi_2Se_3 topological insulator [13, 14, 23].

The pulsed output power attainable from the current Yb:LaCOB/Bi_2Te_3 laser seems moderate. The Q-switching instability arising from thermal effects in the Bi_2Te_3 sample constitutes the major obstacle to further output power scaling. It is essential to reduce the unnecessary, unsaturable absorption and to increase the thermal stability of the 2D Bi_2Te_3 absorber by the improvement in its optical as well as material quality.

4 Conclusions

In summary, efficient passively Q-switched laser operation of Yb:LaCOB at 1071–1080 nm was demonstrated, with 2D Bi_2Te_3 topological insulator acting as saturable absorber. This was also the first time that an Yb-ion laser operating in the long-wavelength region beyond 1.07 µm and passively Q-switched with 2D saturable absorber was realized. A pulsed output power of 1.76 W was generated at 140 kHz with a slope efficiency of 38%, resulting in pulse energy of 12.6 µJ, while the corresponding pulse duration and peak power were 288 ns and 43.8 W, respectively.

References

1. J. Liu, W. Han, H. Zhang, J. Wang, V. Petrov, Appl. Phys. B **91**, 329 (2008)
2. P. Loiko, J.M. Serres, X. Mateos, H. Yu, H. Zhang, J. Liu, K. Yumashev, U. Griebner, V. Petrov, M. Aguiló, F. Díaz, IEEE Photonics J. **8**, 1501312 (2016)
3. J. Liu, H. Yang, H. Zhang, J. Wang, V. Petrov, Appl. Opt. **47**, 5436 (2008)
4. X. Chen, H. Xu, W. Han, H. Yi, H. Yu, H. Zhang, J. Liu, Opt. Laser Technol. **70**, 128 (2015)
5. X. Chen, H. Xu, Y. Guo, W. Han, H. Yu, H. Zhang, J. Liu, Appl. Opt. **54**, 7142 (2015)
6. J. Liu, W. Han, X. Chen, Q. Dai, H. Yu, H. Zhang, IEEE J. Sel. Top. Quantum Electron. **21**, 1600808 (2015)
7. X. Chen, L. Wang, J. Liu, Y. Guo, W. Han, H. Xu, H. Yu, H. Zhang, Opt. Laser Technol. **79**, 74 (2016)
8. X. Chen, W. Han, H. Xu, M. Jia, H. Yu, H. Zhang, J. Liu, Appl. Opt. **54**, 3225 (2015)
9. J. Liu, X. Chen, W. Han, H. Xu, H. Yu, H. Zhang, IEEE Photonics Technol. Lett. **28**, 1104 (2016)
10. X. Chen, L. Wang, W. Han, Y. Guo, H. Xu, H. Yu, H. Zhang, J. Liu, Opt. Express **23**, 30357 (2015)
11. Y. Ma, K. Tian, X. Dou, J. Yang, Y. Li, W. Han, H. Xu, J. Liu, Opt. Express **26**, 25147 (2018)
12. K. Tian, J. Yang, H. Yi, X. Dou, Y. Ma, Y. Li, W. Han, J. Liu, Opt. Laser Technol. **113**, 1 (2019)
13. J. Yang, Y. Ma, K. Tian, Y. Li, X. Dou, W. Han, H. Xu, J. Liu, Opt. Mater. Express **8**, 3146 (2018)
14. J. Yang, Y. Li, K. Tian, F. Liu, X. Dou, Y. Ma, W. Han, H. Xu, J. Liu, Laser Phys. Lett. **15**, 125802 (2018)
15. H.C. Liang, J.Y. Huang, K.W. Su, H.C. Lai, Y.F. Chen, K.F. Huang, H.J. Zhang, J.Y. Wang, M.H. Jiang, Appl. Opt. **46**, 2292 (2007)
16. L. Chen, Z. Wang, H. Yu, S. Zhuang, S. Han, Y. Zhao, X. Xu, Appl. Phys. Express **5**, 112701 (2012)
17. A. Aron, G. Aka, B. Viana, A. Kahn-Harari, D. Vivien, F. Druon, F. Balembois, P. Georges, A. Brun, N. Lenain, M. Jacquet, Opt. Mater. **16**, 181 (2001)
18. F. Mougel, K. Dardenne, G. Aka, A. Kahn-Harari, D. Vivien, J. Opt. Soc. Am. B **16**, 164 (1999)
19. Y. Ji, J. Cao, J. Xu, Z. You, C. Tu, Appl. Opt. **52**, 5079 (2013)
20. Y. Ji, J. Cao, J. Xu, Z. You, C. Tu, Appl. Opt. **53**, 5517 (2014)
21. Y. Li, Y. Xu, G. Xu, L. Dong, X. Dou, J. Liu, Infrared Phys. Technol. **99**, 167 (2019)
22. Y. Ji, J. Cao, C. Tu, Opt. Mater. **35**, 2698 (2013)
23. J. Yang, K. Tian, Y. Li, X. Dou, Y. Ma, W. Han, H. Xu, J. Liu, Opt. Express **26**, 21379 (2018)